Geophysical Research Letters

RESEARCH LETTER
10.1029/2018GL079090

Key Points:
- With the 1-D PIC model, we have investigated the generation of those unusual lower harmonic magnetosonic waves by a proton ring distribution
- The lower harmonic waves are found to be driven by the nonlinear wave-wave couplings of the linearly generated magnetosonic waves
- Our simulations will give some new insights on the evolution of magnetosonic spectra in magnetosphere

Correspondence to:
Q. Lu and L. Chen,
qmlu@ustc.edu.cn;
lunjin.chen@gmail.com

Citation:
Gao, X., Sun, J., Lu, Q., Chen, L., & Wang, S. (2018). Generation of lower harmonic magnetosonic waves through nonlinear wave-wave interactions. *Geophysical Research Letters*, *45*, 8029–8034. https://doi.org/10.1029/2018GL079090

Received 5 JUN 2018
Accepted 1 AUG 2018
Accepted article online 7 AUG 2018
Published online 24 AUG 2018

Generation of Lower Harmonic Magnetosonic Waves Through Nonlinear Wave-Wave Interactions

Xinliang Gao[1,2], Jicheng Sun[1,2], Quanming Lu[1,2], Lunjin Chen[3], and Shui Wang[1,2]

[1]CAS Key Laboratory of Geospace Environment, Department of Geophysics and Planetary Science, University of Science and Technology of China, Hefei, China, [2]Collaborative Innovation Center of Astronautical Science and Technology, Harbin, China, [3]Department of Physics, University of Texas at Dallas, Richardson, TX, USA

Abstract Although magnetosonic waves in the Earth's magnetosphere have been well understood by the linear theory, low harmonic magnetosonic waves, which often lack of free energy, can be unusually present. By employing a 1-D particle-in-cell simulation model, we have investigated the generation of those unusual lower harmonic magnetosonic waves in a plasma containing a proton ring distribution. In our simulation, the higher harmonic magnetosonic waves (from~$9\Omega_h$ to ~$12\Omega_h$) are firstly excited due to the unstable proton ring, which can be well explained by the linear theory. Several lower harmonic magnetosonic waves (below $5\Omega_h$), which well separates away from the higher harmonics, soon appear in the system. Those lower harmonics, which do not have any positive linear growth rates, can be generated by a nonlinear mechanism. The bicoherence analysis demonstrates that there is a strong phase coupling among the unusual lower harmonic magnetosonic waves and the magnetosonic waves generated due to the proton ring, supporting the idea that the lower harmonic waves could be driven by the wave-wave couplings of the generated magnetosonic waves. This wave-wave coupling generation mechanism is further confirmed by another two simulations, where two or three pump magnetosonic waves are initially injected. The lower-frequency waves, that is, the fundamental wave and its second harmonic, are also successfully reproduced due to the nonlinear coupling of pump magnetosonic waves. Our simulations not only propose a potential generation mechanism of unusual lower harmonic magnetosonic waves in the Earth's magnetosphere, but also give some new insights on the evolution of magnetosonic spectra.

Plain Language Summary Over the past decades, the linear or quasi-linear theory has been successfully employed in describing the plasma waves and their interactions with charged particles in the space plasma. However, the unprecedented high-resolution satellite data (THEMIS, VAP, MMS, etc.) have discovered many intriguing phenomena in the Earth's magnetosphere, which are not expected in the linear frame. This is why researchers begin to pay increasing attention to the nonlinear wave-particle and wave-wave interactions in space plasma. Many nonlinear processes related to whistler waves in the Earth's magnetosphere have already been reported and studied. However, there are quite few works about nonlinear physics related to magnetosonic waves. Meanwhile, several lower harmonic magnetosonic waves, with lack of support from the linear instability, are observed in both satellite data and simulations. In this paper, we propose a new idea that the lower harmonic waves could be driven by the wave-wave couplings of the generated magnetosonic waves, which is supported by PIC simulations. This result suggests that the spectrum of magnetosonic waves in the Earth's magnetosphere could be reshaped through nonlinear wave-wave interactions, which ultimately affects the electron dynamics in the Van Allen radiation belt.

1. Introduction

Fast magnetosonic waves, also named as ion Bernstein modes, are highly oblique whistler-mode electromagnetic emissions observed in the Earth's inner magnetosphere between the local proton gyrofrequency and the lower hybrid frequency (Boardsen et al., 2016; Ma et al., 2014). Magnetosonic waves have been widely considered as a significant candidate for the acceleration and pitch angle scattering of radiation belt electrons (Bortnik & Thorne, 2010; Horne et al., 2007; Ma et al., 2016; Ni et al., 2017; Xiao et al., 2015), as well as the energization of background cool protons and electrons (Sun et al., 2017; Yuan et al., 2018). The waves are firstly called equatorial noise by Russell et al. (1970), since they are usually confined within a few degrees of the magnetic equator both inside and outside the plasmapause (Boardsen et al., 2016; Ma et al., 2013). Both satellite observations and the linear theory indicate that such equatorial magnetosonic waves can be

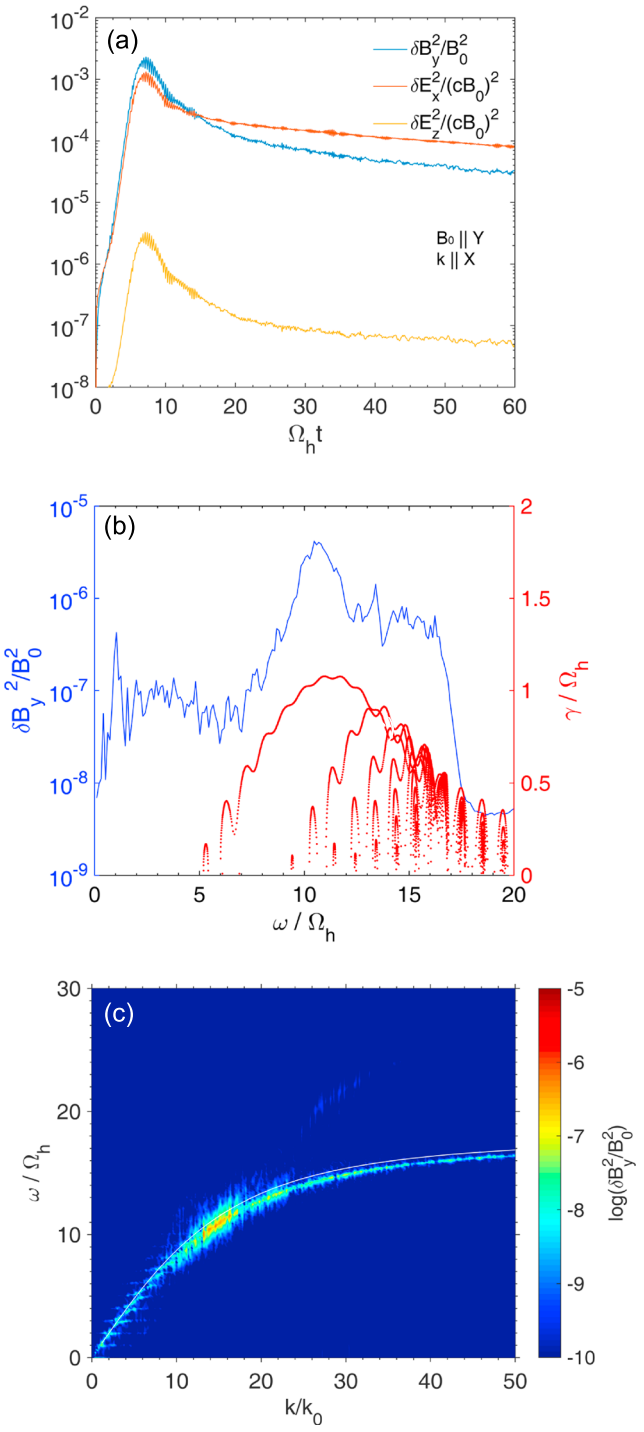

Figure 1. (a) The time profiles of amplitudes of fluctuating magnetic ($\delta B_y^2/B_0^2$) and electric ($\delta E_x^2/(cB_0)^2$ and $\delta E_z^2/(cB_0)^2$) fields. (b) The power spectrum of disturbed magnetic fields $\delta B_y^2/B_0^2$ obtained from the Fourier transform of $\delta B_y(t)/B_0$. The red lines denote the linear growth rates of magnetosonic waves as a function of frequency. (c) The dispersion relation of excited magnetosonic waves. The white line gives the linear dispersion relation of magnetosonic waves in a cold plasma.

generated with the nearly linear polarization of magnetic field perturbations and very large wave normal angles (≈90°) by a natural instability driven by a ring-like distribution of energetic protons with the positive phase space density gradient around the local Alfven speed (Chen et al., 2016; Liu et al., 2011; Ma et al., 2014; Su et al., 2017; Sun, Gao, Chen, et al., 2016; Sun et al., 2017). Moreover, magnetosonic waves in the inner magnetosphere are more typically observed to have a series of narrow tones spaced at multiples of the local proton gyrofrequency (Min et al., 2018; Su et al., 2017; Zhima et al., 2015), while they can also exhibit a continuous spectrum in the dynamic spectrogram (Tsurutani et al., 2014). The discrete and continuous nature of magnetosonic wave instability has been well explored by the linear theory (Chen et al., 2016; Sun, Gao, Chen, et al., 2016) and particle-in-cell (PIC) simulations (Sun, Gao, Lu, et al., 2016).

Although the linear theory is capable of interpreting many observed properties of magnetosonic waves, there are also some intriguing phenomena beyond its scope. Based on THEMIS (Time History of Events and Macroscale Interactions during Substorms) observations, Fu et al. (2014) have reported several rising-tone magnetosonic waves, whose elements are found to be quasi-periodically repeated. Since they morphologically resemble rising-tone chorus waves, their generation may be also related to the nonlinear trapping of charged particles. Moreover, Su et al. (2017) found that within one event, besides the usual magnetosonic waves at higher harmonics, there are also significant wave power at the fundamental and second harmonics. The magnetosonic event analyzed in Min et al. (2018) later presented a single fourth harmonic of the proton gyrofrequency well separated from a main band of higher harmonics continuously ranging from 8th to 32nd. Linear analysis using observed parameters account for the generation of the main band but not for the lower harmonics (Min et al., 2018; Su et al., 2017). Such disagreement between the appearance of lower harmonics and the lack of linear instability for them has been also shown previously in simulation results (Sun, Gao, Lu, et al., 2016; Sun et al., 2017). In this letter, with a one-dimensional (1-D) PIC simulation model, we demonstrate that the magnetosonic waves at lower harmonics are excited by the nonlinear couplings of higher harmonic magnetosonic waves.

2. Simulation Model and Initial Setup

The PIC simulation model is a powerful tool to study nonlinear physical processes in space plasma (Chen et al., 2017; Fu et al., 2017; Gao et al., 2017; Ke et al., 2017), where the electromagnetic fields are updated by solving Maxwell equations and the positions and velocities of ions and electrons are advanced by solving relativistic motions in the electromagnetic fields. A 1-D PIC simulation model with periodic boundary conditions is utilized to study the nonlinear wave-wave interactions of magnetosonic waves, which retains three-dimensional electromagnetic fields and particle velocities but only 1-D spatial variations along the *x* axis. The background magnetic field $\mathbf{B_0}$ lies along the *y* axis, and the waves are assumed to propagate along the *x* axis, which is perpendicular to the background magnetic field. The simulation model is performed in a homogenous and collisionless plasma, which consists of cool protons, cool electrons, and ring-distribution protons. A rather realistic mass ratio between proton and electron $m_h/m_e = 1{,}600$ is adopted. Cool protons and electrons have the same temperature, and the thermal velocity of cool protons is initially

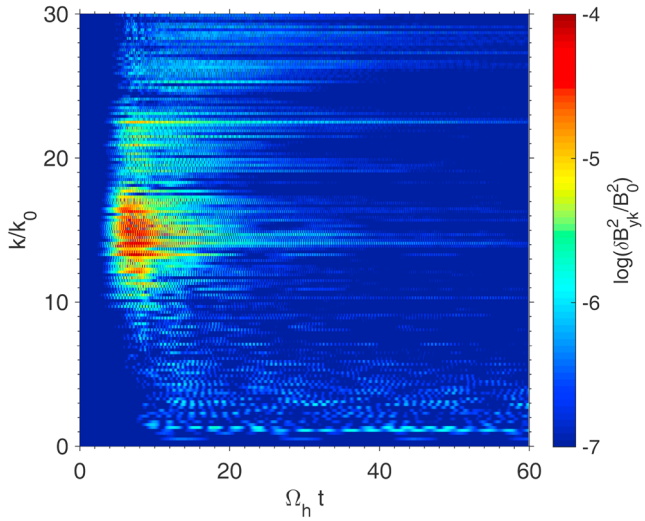

Figure 2. The *k-t* spectrogram of $\delta B_y^2/B_0^2$.

set as $0.00635V_A$ (V_A is the Alfven speed). The distribution function of ring-distribution protons is given by an ideal ring distribution function $f_{hr} = n_{hr}\delta(v_\parallel)\delta(v_\perp - V_R)/(2\pi v_\perp)$, where $v_\parallel$ and $v_\perp$ are velocities parallel and perpendicular to the background magnetic field, n_{hr}(=$0.05n_e$) is the number density, and V_R (=V_A) is the proton ring velocity. The choice of such ideal ring distribution is not critical since it is used for exciting proton cyclotron harmonics. In the simulation model, the time and space have been normalized by the inverse of proton gyrofrequency Ω_h^{-1} and proton inertial length λ_i ($\lambda_i = c/\omega_{ph}$, where c and ω_{ph} are the light speed and proton plasma frequency), respectively. Here a smaller value for light speed $c = 20V_A$ is chosen just to save computation resources. The number of grid cells is $n_x = 32768$, and the grid size is $\Delta x = 9.59 \times 10^{-4}\lambda_i$. For each species, there are on average 100 superparticles per cell. The time step is $\Delta t = 0.05\Omega_e^{-1}$.

3. Simulation Results

Figure 1a shows temporal evolution of amplitudes of fluctuating magnetic and electric fields. The ring-distribution protons are unstable to excite magnetosonic waves, whose magnetic amplitude $\delta B_y^2/B_0^2$ gains a rapid increase from the very beginning and reaches its peak (~$3\times10^{-3}B_0^2$) at about $8\Omega_h^{-1}$. The dominant wave power is found in δB_y and δE_x, which is consistent with the polarization of perpendicular magnetosonic waves. Figure 1b presents the power spectrum of disturbed magnetic fields $\delta B_y^2/B_0^2$ obtained by performing the Fourier transform in time of $\delta B_y/B_0$ at every spatial cell and then averaging over all spatial cells. Besides, the linear growth rate of magnetosonic waves as a function of frequency is also over plotted in Figure 1b, which is calculated by employing the initial plasma condition and the theoretical model used in Chen et al. (2016). As shown in Figure 1b, the generated magnetosonic waves exhibit a continuous spectrum over the frequency range of ~7–$16\Omega_h$ with a clear power peak at about $11\Omega_h$. The continuous spectrum is well predicted by the linear theory in that the linear growth rates exhibit a quite similar frequency range to the simulated spectrum and the peak growth rate occurs at the similar frequency corresponding to the peak of the simulated spectrum. Surprisingly, there exists significant although weaker magnetic power at the lower harmonics (1–$5\Omega_h$) with another peak at the fundamental proton gyrofrequency. According to the linear theory, however, no positive growth rates are obtained for these lower-frequencies wave modes (Figure 1b). Figure 1c shows the power distribution in the frequency and wavenumber domain. The excited power agrees very well with the dispersion relation of magnetosonic waves (white line). The dominant wave modes with a continuous spectrum mainly concentrates in the range of $9\Omega_h \le \omega \le 12\Omega_h$ and $11k_0 \le k \le 17k_0$ (where $k_0 = \lambda_i^{-1}$). However, magnetosonic waves with lower frequencies ($<5\Omega_h$) exhibit a discrete spectrum and have significant magnetic power just at the lower harmonics including the fundamental. We also note that there exist the second harmonic of those dominant pump magnetosonic waves ($20\Omega_h \le \omega \le 25\Omega_h$, $22k_0 < k < 34k_0$), despite quite weak and substantially deviated away from the dispersion relation curve (the white line of Figure 1c).

Figure 2 illustrates the *k-t* spectrogram of $\delta B_y/B_0$, which clearly presents the time evolution of the magnetosonic wave spectrum. As shown in Figure 2, during an initial interval of about $8\Omega_h^{-1}$, the magnetic fluctuations rapidly grow up to their peak amplitudes, with a broad band spectrum above ~$10k_0$ and peak at ~$15k_0$. These higher-frequency magnetic fluctuations are just magnetosonic waves excited by the initial ring-distribution protons, which can be well explained by the linear theory. Note that there is still no observable magnetic power below $5\Omega_h$. Subsequently, the higher-frequency magnetosonic waves are found to gradually decay, which primarily resulted from the scattering of proton ring-distribution toward less unstable distribution and the energization of cool protons and electrons. More importantly, the magnetic fluctuations at the proton gyrofrequency and its lower harmonics (below $5\Omega_h$) begin to grow from the noise level, and reaches their peak power at about $18\Omega_h^{-1}$. Besides, these magnetosonic waves at lower frequencies can persist for a very long time in this system, even when the higher-frequency waves become very weak at later time. We have checked the linear grow rate of the system at the beginning of the growth phase of magnetic fluctuations at lower frequencies (at $t = 9\Omega_h^{-1}$), and found that the linear

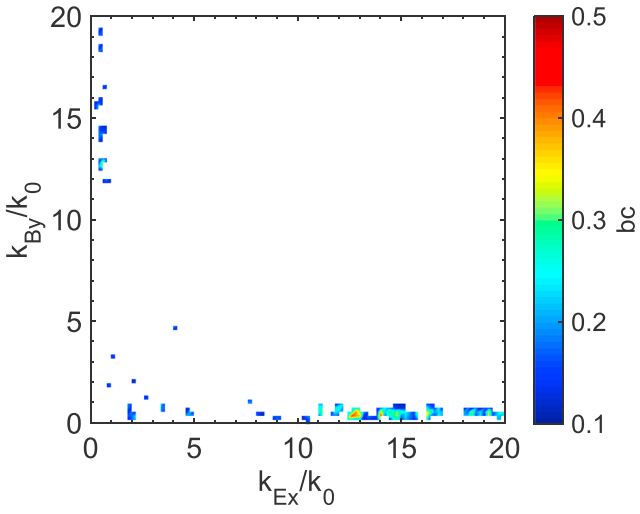

Figure 3. The distribution of bicoherence indices in the (k_{Ex}, k_{By}) plane.

growth rate below $5\Omega_h$ is still zero (neutral mode), which explain long lifetime of those emission after excited. Below, we demonstrate that the unexpected magnetosonic waves at the lower harmonics including the fundamental are driven through the nonlinear wave-wave interactions of higher-frequency waves that are excited by the proton ring distribution.

The bicoherence analysis is a widely used method to identify the underlying wave-wave interactions in a plasma system. The analysis can measure the phase relation among three magnetosonic waves (Gao et al., 2014, 2017; Milligen et al., 1995). Here we choose the parallel component of fluctuating magnetic fields δB_y at two wavenumbers k_{By} and k_w and one perpendicular component of electric fields δE_x at the wavenumber $k_w = k_{Ex} + k_{By}$ to calculate the bicoherence index, which is defined as

$$\mathrm{bc}(k_{Ex}, k_{By}) = \frac{\left|\left\langle \delta E_x(k_{Ex})\delta B_y(k_{By})\delta B_y^*(k_w)\right\rangle\right|^2}{\left\langle\left|\delta E_x(k_{Ex})\delta B_y(k_{By})\right|^2\right\rangle\left\langle\left|\delta B_y^*(k_w)\right|^2\right\rangle},$$

where the bracket $\langle\ \rangle$ denotes an average over the time interval of 10–20 Ω_h^{-1}. Figure 3 presents the distribution of bicoherence indices in the (k_{Ex}, k_{By}) plane. Note that the large bicoherence index (close to 1) indicates the three wave modes satisfy the wavenumber resonant condition. In Figure 3, relatively large bicoherence indices (0.3–0.5) are only found in the range of ($11 - 15k_0$, $1k_0$), suggesting there are strong coupling processes among the fundamental mode and dominant magnetosonic waves generated by the proton ring. It is worth noting that the bicoherence indices for wave modes at lower harmonics (2–$5\Omega_h$) are quite small, because their small amplitudes relative to the background noise makes the phase measurement highly error prone.

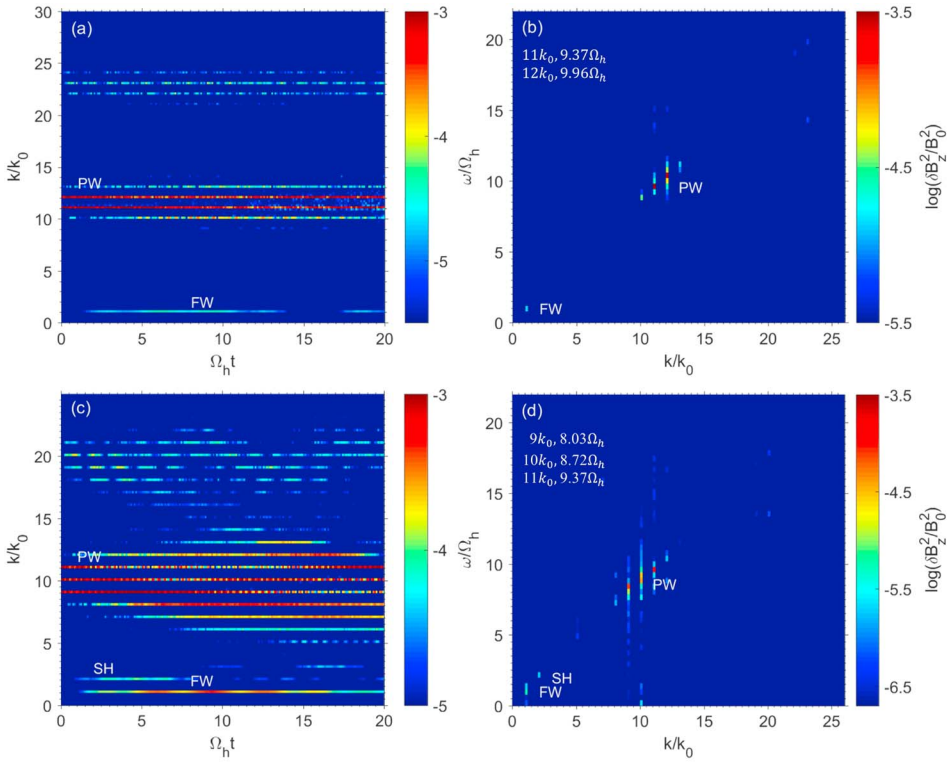

Figure 4. (a, c) The *k-t* spectrum of $\delta B_z^2/B_0^2$ and (b, d) the dispersion relation of magnetic fluctuations. In all panels, *FW*, *SH*, and *PW* stand for the fundamental wave, second harmonic of the fundamental wave, and pump magnetosonic waves, respectively. The wave numbers and frequencies of pump magnetosonic waves are listed in (b) and (d).

To support the proposed generation mechanism of the magnetosonic waves at lower frequencies, we further perform another two simulation runs by injecting magnetosonic waves at higher harmonics instead of generating them through the instability of proton ring distribution. In both simulation runs, there are only cool protons and electrons in the plasma system, and the pump magnetosonic waves are initially launched in the simulation box. Following a similar method to Gao et al. (2017), the pump magnetosonic waves are set up by assigning fluctuating wave fields on each grid and fluctuating bulk velocity to each particle based on the linear theory model (Chen et al., 2016). In the first simulation run, two pump waves are chosen with wave number and frequency pairs of ($11k_0$, $9.37\Omega_h$) and ($12k_0$, $9.96\Omega_h$), respectively, so that the separation in wave number is $1k_0$. We use *FW*, *SH* and *PW* to stand for the fundamental wave, the second harmonic of FW, and pump waves, respectively. Figure 4a shows the *k-t* spectrum of $\delta B_z^2/B_0^2$, and the dispersion relation is given in Figure 4b. As time increases, there are many more wave modes appearing in this system besides two initially injected pump magnetosonic waves (Figure 4a). Since the two pump magnetosonic waves are carefully designed to have wave numbers with a difference of $1k_0$, then the fundamental wave mode ($1k_0$) will be generated through the coupling between two pump waves as shown in Figure 4b. Meanwhile, other waves are also observed, such as side-band waves ($10k_0$ and $13k_0$) just above and below the pump waves and the higher-frequency waves ($>20k_0$ and $>18\Omega_h$), near the second harmonic of pump waves. In the same format, Figures 4c and 4d display the result for the second simulation run, where three pump waves ($9k_0$, $8.03\Omega_h$; $10k_0$, $8.72\Omega_h$; $11k_0$, $9.37\Omega_h$) are initially launched. Just as expected, not only the fundamental wave mode ($1k_0$) is excited in this plasma system, but also the second harmonic (i.e., $2k_0$) is driven by the pump waves (Figures 4c and 4d). This result will support that those lower-frequency magnetosonic waves without positive linear growth rate can be driven by the magnetosonic waves with positive linear grow rate. Furthermore, nonlinear wave-wave coupling process significantly increases the number of harmonic lines.

4. Conclusion and Discussion

By employing 1-D PIC simulation model, we have investigated the generation of lower harmonic magnetosonic waves, which have been reported both in observational and simulation works (Min et al., 2018; Su et al., 2017; Sun, Gao, Lu, et al., 2016; Sun et al., 2017). In our simulation, the higher harmonic magnetosonic waves (from~$9\Omega_h$ to ~$12\Omega_h$) are initially excited due to the unstable proton ring and are quite consistent with the linear theory. The appearance of lower harmonics waves ($<5\Omega_h$), as the simulation proceeds, is not predicted from the linear theory. The bicoherence analysis demonstrates that there is a strong phase coupling among the lower harmonic magnetosonic waves and those linearly generated magnetosonic waves, supporting the lower harmonic waves could be driven by the wave-wave couplings of those linearly generated magnetosonic waves. This generation mechanism is further confirmed by another two simulations, where the pump magnetosonic waves are initially injected. Due to their strong coupling, the lower harmonic waves (including the fundamental wave), side-band waves, and second harmonic of each pump wave are all excited in this system.

The simulation model in this study, although being a closed system, does provide implication for the realistic open system. As shown in Figures 4b and 4d, the group velocity of pump magnetosonic waves is roughly 1 V_A, and the total length of the simulation box is given as 31.4 V_A/Ω_h. Therefore, the time T_0 to across the simulation box is estimated as $31.4\Omega_h^{-1}$, which is much larger than the time scale of fundamental wave excitation (~$2\Omega_h^{-1}$). This means there is enough time for driving the FW once those pump waves are excited. In an open system, the pump waves need to propagate in the same direction in order for nonlinear wave-wave coupling to be more effective because of the linear relation between ω and **k**. The scenario of the same propagation direction is possible because waves tend to experience convective growth over a longer distance in the azimuthal direction and thus obtain larger wave gain in the azimuthal direction. We note that many parameters (i.e., the background magnetic field, electron density, abundance of ring protons, and wave normal angle) may influence the linear growth rates and spectral structures of those magnetosonic waves generated by the proton ring and may ultimately affect the nonlinear excitation of lower harmonic waves. The dependence on those parameters requires a full study, and will be investigated in detail as a future work.

Magnetosonic waves in the Earth's magnetosphere are commonly believed to be generated by the energetic ring-distribution protons. Linear instability of such proton ring has been demonstrated by both simulations and observations (Chen et al., 2016; Liu et al., 2011; Ma et al., 2014; Yuan et al., 2018). However, several

lower harmonic magnetosonic waves, not predicted by the linear theory, are also observed. Based on our simulations, it is clearly shown that the lower harmonic magnetosonic waves will be driven just after the linearly generated waves obtain sufficiently large amplitudes. We further find that these lower harmonic waves are strongly coupled with those linearly generated magnetosonic waves, supporting that their generation can be caused by the nonlinear wave-wave interactions. Our study implies the spectra of magnetosonic waves in the Earth's magnetosphere could be reshaped through nonlinear wave-wave interactions, which ultimately affects the electron dynamics in the Van Allen radiation belt. In summary, our simulations not only propose a potential generation mechanism of lower harmonic magnetosonic waves in the Earth's magnetosphere, but also give some new insights on the evolution of magnetosonic spectra.

Acknowledgments
This work was supported by the NSFC Grants 41527804, 41604128, 41774151, and 41631071; Youth Innovation Promotion Association of Chinese Academy of Sciences (No. 2016395); and Key Research Program of Frontier Sciences, CAS (QYZDJ-SSW-DQC010). LC acknowledges the NSF Grants 1405041 and 1705079 through the Geospace Environment Modeling program. The simulation data will be preserved on a long-term storage system and will be made available upon request to the corresponding authors (https://share.weiyun.com/56qg3Nl).

References

Boardsen, S. A., Hospodarsky, G. B., Kletzing, C. A., Engebretson, M. J., Pfaff, R. F., Wygant, J. R., et al. (2016). Survey of the frequency dependent latitudinal distribution of the fast magnetosonic wave mode from Van Allen Probes Electric and Magnetic Field Instrument and Integrated Science waveform receiver plasma wave analysis. *Journal of Geophysical Research: Space Physics*, *121*, 2902–2921. https://doi.org/10.1002/2015JA021844

Bortnik, J., & Thorne, R. M. (2010). Transit time scattering of energetic electrons due to equatorially confined magnetosonic waves. *Journal of Geophysical Research*, *115*(A7), A07213. https://doi.org/10.1029/2010JA015283.

Chen, H., Gao, X., Lu, Q., Ke, Y., & Wang, S. (2017). Lower band cascade of whistler waves excited by anisotropic hot electrons: One-dimensional PIC simulations. *Journal of Geophysical Research: Space Physics*, *122*, 10,448–10,457. https://doi.org/10.1002/2017JA024513.

Chen, L. J., Sun, J. C., Lu, Q. M., Gao, X. L., Xia, Z. Y., & Zhima, Z. (2016). Generation of magnetosonic waves over a continuous spectrum. *Journal of Geophysical Research: Space Physics*, *121*, 1137–1147. https://doi.org/10.1002/2015JA022089

Fu, H. S., Cao, J. B., Zhima, Z., Khotyaintsev, Y. V., Angelopoulos, V., Santolik, O., et al. (2014). First observation of rising-tone magnetosonic waves. *Geophysical Research Letters*, *41*, 7419–7426. https://doi.org/10.1002/2014GL061867

Fu, X., Gary, S. P., Reeves, G. D., Winske, D., & Woodroffe, J. R. (2017). Generation of highly oblique lower band chorus via nonlinear three-wave resonance. *Geophysical Research Letters*, *44*, 9532–9538. https://doi.org/10.1002/2017GL074411

Gao, X., Ke, Y., Lu, Q., Chen, L., & Wang, S. (2017). Generation of multiband chorus in the Earth's magnetosphere: 1-D PIC simulation. *Geophysical Research Letters*, *44*(2), 618–624. https://doi.org/10.1002/2016GL072251

Gao, X. L., Lu, Q. M., Li, X., Hao, Y. F., Tao, X., & Wang, S. (2014). Ion dynamics during the parametric instabilities of a left-hand polarized Alfvén wave in a proton-electron-alpha plasma. *The Astrophysical Journal*, *780*(1), 56.

Horne, R. B., Thorne, R. M., Glauert, S. A., Meredith, N. P., Pokhotelov, D., & Santolik, O. (2007). Electron acceleration in the Van Allen radiation belts by fast magnetosonic waves. *Geophysical Research Letters*, *34*, L17107. https://doi.org/10.1029/2007GL030267

Ke, Y., Gao, X., Lu, Q., & Wang, S. (2017). Parametric decay of a parallel propagating monochromatic whistler wave: Particle-in-cell simulations. *Physics of Plasmas*, *24*(1), 012108. https://doi.org/10.1063/1.4974160

Liu, K. J., Gary, S. P., & Winske, D. (2011). Excitation of magnetosonic waves in the terrestrial magnetosphere: Particle-in-cell simulations. *Journal of Geophysical Research*, *116*, A07212. https://doi.org/10.1029/2010JA016372

Ma, Q. L., Li, W., Chen, L. J., Thorne, R. M., & Angelopoulos, V. (2014). Magnetosonic wave excitation by ion ring distributions in the Earth's inner magnetosphere. *Journal of Geophysical Research: Space Physics*, *119*, 844–852. https://doi.org/10.1002/2013JA019591

Ma, Q. L., Li, W., Thorne, R. M., & Angelopoulos, V. (2013). Global distribution of equatorial magnetosonic waves observed by THEMIS. *Geophysical Research Letters*, *40*(10), 1895–1901. https://doi.org/10.1002/grl.50434

Ma, Q. L., Li, W., Thorne, R. M., Bortnik, J., Kletzing, C. A., Kurth, W. S., & Hospodarsky, G. B. (2016). Electron scattering by magnetosonic waves in the inner magnetosphere. *Journal of Geophysical Research: Space Physics*, *121*, 274–285. https://doi.org/10.1002/2015JA021992

Milligen, B. P. V., Sánchez, E., Estrada, T., Hidalgo, C., Brañas, B., Carreras, B., & García, L. (1995). Wavelet bicoherence: A new turbulence analysis tool. *Physics of Plasmas*, *2*(8), 3017–3032. https://doi.org/10.1063/1.871199

Min, K., Liu, K., Wang, X., Chen, L., & Denton, R. E. (2018). Fast magnetosonic waves observed by Van Allen Probes: Testing local wave excitation mechanism. *Journal of Geophysical Research: Space Physics*, *123*, 497–512. https://doi.org/10.1002/2017JA024867

Ni, B. B., Hua, M., Zhou, R. X., Yi, J., & Fu, S. (2017). Competition between outer zone electron scattering by plasmaspheric hiss and magnetosonic waves. *Geophysical Research Letters*, *44*(8), 3465–3474. https://doi.org/10.1002/2017GL072989

Russell, C. T., Holzer, R. E., & Smith, E. J. (1970). OGO 3 observations of ELF noise in the magnetosphere: 2. The nature of the equatorial noise. *Journal of Geophysical Research*, *75*(4), 755–768. https://doi.org/10.1029/JA075i004p00755

Su, Z. P., Wang, G., Liu, N. G., Zheng, H. N., Wang, Y. M., & Wang, S. (2017). Direct observation of generation and propagation of magnetosonic waves following substorm injection. *Geophysical Research Letters*, *44*(15), 7587–7597. https://doi.org/10.1002/2017GL074362

Sun, J. C., Gao, X. L., Chen, L. J., Lu, Q. M., Tao, X., & Wang, S. I. (2016). A parametric study for the generation of ion Bernstein modes from a discrete spectrum to a continuous one in the inner magnetosphere. I. Linear theory. *Physics of Plasmas*, *23*(2), 022901.

Sun, J. C., Gao, X. L., Lu, Q. M., Chen, L. J., Liu, X., Wang, X. Y., et al. (2017). Spectral properties and associated plasma energization by magnetosonic waves in the Earth's magnetosphere: Particle-in-cell simulations. *Journal of Geophysical Research: Space Physics*, *122*, 5377–5390. https://doi.org/10.1002/2017JA024027

Sun, J. C., Gao, X. L., Lu, Q. M., Chen, L. J., Tao, X., & Wang, S. I. (2016). A parametric study for the generation of ion Bernstein modes from a discrete spectrum to a continuous one in the inner magnetosphere. II. Particle-in-cell simulations. *Physics of Plasmas*, *23*(2), 022902.

Tsurutani, B. T., Falkowski, B. J., Pickett, J. S., Verkhoglyadova, O. P., Santolik, O., & Lakhina, G. S. (2014). Extremely intense ELF magnetosonic waves: A survey of polar observations. *Journal of Geophysical Research: Space Physics*, *119*, 964–977. https://doi.org/10.1002/2013JA019284

Xiao, F. L., Yang, C., Su, Z. P., Zhou, Q. H., He, Z. G., He, Y. H., et al. (2015). Wave-driven butterfly distribution of Van Allen belt relativistic electrons. *Nature Communications*, *6*(1), 8590. https://doi.org/10.1038/ncomms9590

Yuan, Z., Yu, X., Huang, S., Qiao, Z., Yao, F., & Funsten, H. O. (2018). Cold ion heating by magnetosonic waves in a density cavity of the plasmasphere. *Journal of Geophysical Research: Space Physics*, *123*, 1242–1250. https://doi.org/10.1002/2017JA024919

Zhima, Z., Chen, L. J., Fu, H. S., Cao, J. B., Horne, R. B., & Reeves, G. (2015). Observations of discrete magnetosonic waves off the magnetic equator. *Geophysical Research Letters*, *42*(22), 9694–9701. https://doi.org/10.1002/2015GL066255